SYNTHESIS, CHARACTERIZATION AND ELECTROCHEMICAL BEHAVIOR OF SOME Mo(V)-Sn(II) COMPLEX COMPOUNDS

Haritina CHIVU[1], Denisa FICAI[2], Magdalena Rodica BUJDUVEANU[3], Vasile BERCU[4], Olimpia MICU[5], Eleonora-Mihaela UNGUREANU[6], Cornelia GURAN[7]

*În acest articol se prezintă rezultatele obţinute de noi asupra sistemelor Mo(V): $SnCl_2$: **L**, în care **L** reprezintă un derivat de piridazonă (6-p-tolil-2H-piridazin-3-onă şi 6-(4-cloro-fenil)-2H-piridazin-3-onă) sau 2,4,6-triamino-[1,3,5]-triazină. Compuşii mononucleari au fost obţinuţi pornind de la Mo(VI) şi $SnCl_2$. $SnCl_2$ acţionează atât ca reducător faţă de Mo(VI) cât şi ca ligand. Au fost izolate specii mononucleare $(\mathbf{L}H)_2[MoOCl_4(SnCl_3)]$, care conţin unitatea $SnCl_3^-$ ca ligand. Acesti compuşi, au fost caracterizaţi prin analiză chimică elementală, spectroscopie IR, UV-Vis şi RES, conductivitate electrică molară. Combinaţiile complexe obţinute, $(\mathbf{L}H)_2[MoOCl_4(SnCl_3)]$, au structuri monomere şi geometrii octaedrice. Liganzii organici **L** acţionează ca specii monoprotonate, $\mathbf{L}H^+$ în toţi compuşii obţinuţi. S-au investigat proprietăţile electrochimice ale liganzilor şi combinaţiilor complexe $(\mathbf{L}H)_2[MoOCl_4(SnCl_3)]$ prin voltametrie ciclică şi voltametrie puls-diferenţială.*

*The results obtained in our studies on the Mo(V): $SnCl_2$: **L** systems, in which **L** is either a pyridazone derivative (6-p-tolyl-2H-pyridazine-3-one, 6-(4-chloro-phenyl)-2H-pyridazine-3-one) or 2,4,6-triamine-[1,3,5]-triazine are reported in this article. Mononuclear complex compounds have been synthesized starting from Mo(VI) and $SnCl_2$. $SnCl_2$ acted not only as a reducing agent toward Mo(VI), but also as ligand. Mononuclear species $(\mathbf{L}H)_2[MoOCL_4(SnCl_3)]$, containing $SnCl_3^-$ unit as ligand have been isolated. These compounds were characterized by elemental analysis, IR, UV-Vis and EPR spectra, and molar electrical conductivitiy. The*

[1] PhD Student, Department of Inorganic Chemistry, University POLITEHNICA of Bucharest, Romania, hari_chivu@yahoo.com

[2] Assistant Prof., Department of Inorganic Chemistry, University POLITEHNICA of Bucharest, , Romania manzu_denisa76@yahoo.com

[3] PhD Student, Department of Applied Physical Chemistry and Electrochemistry, University POLITEHNICA of Bucharest, Romania, m_bujduveanu@yahoo.com.

[4] Assistant Prof., Department of Atomic and Nuclear Physics, University of Bucharest, P.O.boxmg-11, 077125 Magurele, vbercu@gmail.com.

[5] Prof., Department of Inorganic Chemistry, University POLITEHNICA of Bucharest, Romania, o.micu@yahoo.com

[6] Prof., Department of Applied Physical Chemistry and Electrochemistry, University POLITEHNICA of Bucharest, Romania, em_ungureanu2000@yahoo.com

[7] Prof., Department of Inorganic Chemistry, University POLITEHNICA of Bucharest, Romania, cornelia_guran@yahoo.com

obtained complex ($\mathbf{L}H)_2[MoOCl_4(SnCl_3)]$ compounds have monomeric structure and octahedral geometry. The organic ligands **L** *act as monoprotonated species,* $\mathbf{L}H^+$ *in all the obtained complex compounds. Electrochemical properties of the ligands and their complex compounds ($\mathbf{L}H)_2[MoOCl_4(SnCl_3)]$ were investigated by cyclic voltammetry and differential pulse voltammetry.*

Keywords: oxomolybdenum complex compounds, 6-p-tolyl-2H-pyridazine-3-one, 6-(4-chloro-phenyl)-2H-pyridazine-3-one, 2,4,6-triamine-[1,3,5]-triazine, cyclic voltammetry, differential pulse voltammetry

1. Introduction

Higher oxidation state molybdenum complex compounds are well known for their useful applications in industrial redox processes (epoxidation or metathesis of olefins, isomerization of unsaturated alcohols) [1-3]. Some complexes possess a certain capacity to form surface films and to be used as sensors in modern technologies. Oxomolybdenum complex compounds are the dominant type especially for the oxidation state (V) and according to the literature data, there is equilibrium between monomeric $[MoOBr_4]^-$, $[MoOBr_5]^{2-}$, $[MoOBr_4(OH_2)]^-$ and dimeric $[Mo_2O_2(OH)_4Br_4]^{2-}$, $[Mo_2O_3Br_8]^{4-}$, $[Mo_2O_4Br_4(H_2O)_2]^{2-}$ or $[Mo_2O_4Br_2(H_2O)_4]$ Mo(V) species [4-13]. In other works we reported the synthesis and characterization of several oxomolybdenum(V) species as monomers or dimers, with biguanidine, piridazine or *s*-triazine derivatives [14-19].

In this work we report our studies on the Mo(V):$SnCl_2$:**L** systems, in which **L** are pyridazone derivatives (6-p-tolyl-2H-pyridazine-3-one, $\mathbf{L^1}$, 6-(4-chloro-phenyl)-2H-pyridazine-3-one, $\mathbf{L^2}$) or an *s*-triazine derivative (2,4,6-triamine-[1,3,5]-triazine, $\mathbf{L^3}$).

Mononuclear complex compounds have been synthesized starting from $(NH_4)_6Mo_7O_{24}\cdot 12H_2O$ and $SnCl_2\cdot 2H_2O$. As a result, $SnCl_2$ acted not only as a reducing agent toward Mo(VI), but also as ligand. In well established conditions mononuclear species, **1-3**, $(\mathbf{L}H)_2[MoOCl_4(SnCl_3)]$ were isolated, containing the unit $SnCl_3^-$ as ligand.

Based on the elemental chemical analysis, molar electrical conductivity, UV-Vis, IR and EPR spectra for the complex compounds the following formulas have been proposed:

$(\mathbf{L^1}H)_2[MoOCl_4(SnCl_3)]$ **1**

$(\mathbf{L^2}H)_2[MoOCl_4(SnCl_3)]$ **2**

$(\mathbf{L^3}H)_2[MoOCl_4(SnCl_3)]$ **3**

Their electrochemical behavior has been investigated by cyclic voltammetry (CV) and differential pulse voltammetry (DPV).

2. Experimental

Reagents, Instrumentation and Methods

The metallic salts $(NH_4)_6Mo_7O_{24}\cdot 12H_2O$ and $SnCl_2\cdot 2H_2O$, hydrochloric acid and the ligands were purchased from Merck and used without further purification. Acetonitrile (Rathburn, HPLC grade), tetra-*n*-butylammonium perchlorate (TBAP) from Fluka were used as received for solvent and supporting electrolytes.

The complex synthesis was performed in capsules under electrical heating and magnetic stirring.

Nitrogen content was analyzed by Dumas microcombustion (in the usual closed system and CO_2 atmosphere).

The electronic spectra were recorded on a Jasco V560 in diffuse reflectance technique. *EPR spectra* were registered on JEOL JES-FA spectrophotometer.

Infrared vibration spectra were recorded with a Bruker Equinox 55 spectrophotometer. *Molar electrical conductivities* were determined with OK 102/1 Radelkis Conductometer.

Electrochemical experiments were conducted in a conventional three-electrode cell under argon atmosphere at 25°C using a PGSTAT 12 AUTOLAB potentiostat and a PAR 283 potentiostat. The working electrode was a glassy carbon disk (3-mm diameter from Metrohm) polished with 0.1μm diamond paste. The Ag/10mM $AgNO_3$ in CH_3CN + 0.1M TBAP system was used as reference electrode. All potentials were referred to the potential of ferrocene/ferricinium (Fc/Fc^+), which was 0.07V with our experimental conditions. CV experiments were usually performed at 0.1 V/s, and with different scan rates (0.1–1V/s), for investigation of scan rate influence. DPV curves were recorded at 10mV/s with a pulse height of 25mV and a step time of 0.2s.

Complex Compounds Synthesis

The complex compounds $(\mathbf{L}H)_2[MoOCl_4(SnCl_3)]$ **1 – 3** , where **L** was $\mathbf{L^1}$ = 6-p-tolyl-2H-pyridamine-3-one, $\mathbf{L^2}$ = 6-(4-chloro-phenyl)-2H-pyridazine-3-one and $\mathbf{L^3}$ = 2,4,6-triamine-[1,3,5]-triazine, where obtained following the procedure: solutions of 0.5g (0.36mmoles) $(NH_4)_6Mo_7O_{24}\cdot 12H_2O$ in 10mL concentrated hydrochloric acid (1), 0.162g (0.72mmoles) $SnCl_2$ in 10mL concentrated

hydrochloric acid (2) were mixed. The brown – green solutions were left at ambient conditions for 2 days and then were treated with the ethanol solutions of the organic ligand (0.36mmoles organic ligand was solved in 10mL solution of concentrated hydrochloric acid: water: ethanol 1:1:1). By evaporation of the mixed solutions, the monomeric compounds have been obtained as green powders. The elemental analysis results, the values of molar electrical conductivity and IR and UV-Vis main peaks are the following:

1. $(\mathbf{L^1}H)_2[MoOCl_4(SnCl_3)]$

Calculated for $\mathbf{C_{22}H_{20}N_4O_3Cl_7MoSn}$: according to Table 1
Molar electrical conductivity: 182 $\mu S \cdot cm^{-1} \cdot mol^{-1}$ *(methanol solution)* – 1:2 electrolyte
IR (cm^{-1}): $\nu_{N-H,}$ 3200, ν_{OH} = 3350-3150 (w), δ_{N-H} =1660 (m), ν_{C-N} =1400, $\delta_{CH2sym/asym,OH}$ = 1440 (m) ν_{M-N} = 275. ν_{Mo-Sn}= 420, $\nu_{Mo=O}$ =990, ν_{Sn-Cl}= 300
UV/Vis (kK): 33.00, 27.70, 23.20, 14.20

2. $(\mathbf{L^2}H)_2[MoOCl_4(SnCl_3)]$

Calculated for $\mathbf{C_{20}H_{20}N_4O_3Cl_8MoSn:}$ according to Table 1
Molar electrical conductivity: 210 $\mu S \cdot cm^{-1} \cdot mol^{-1}$ *(methanol solution)* – 1:2 electrolyte
IR (cm^{-1}): $\nu_{N-H,}$ 3450, ν_{OH} = 3350-3150 (w), δ_{N-H} =1660 (m), ν_{C-N} = 1410, $\delta_{CH2sym/asym,OH}$ = 1450 (m) ν_{M-N} = 275. ν_{Mo-Sn}= 420, $\nu_{Mo=O}$ = 980, ν_{Sn-Cl} = 300
UV/Vis (kK): 38.00, 27.75, 23.25, 14.30

3. $(\mathbf{L^3}H)_2[MoOCl_4(SnCl_3)]$

Calculated for $\mathbf{C_6H_{14}N_{12}OCl_7MoSn:}$ according to Table 1
Molar electrical conductivity: 196 $\mu S \cdot cm^{-1} \cdot mol^{-1}$ *(methanol solution)* – 1:2 electrolyte
IR (cm^{-1}): $\nu_{N-H,}$ 3120, ν_{OH} = 3350-3150 (w), δ_{N-H} =1670 (m), ν_{C-N} =1400, $\delta_{CH2sym/asym,OH}$ = 1440 (m) ν_{M-N} = 275. ν_{Mo-Sn}=440, $\nu_{Mo=O}$ = 980, ν_{Sn-Cl} = 310
UV/Vis (kK): 33.90, 27.70, 23.30, 14.20.

3. Results and discussion

3.1. Complex compounds synthesis

Starting from the organic ligands, (6-p-tolyl-2H-pyridazine-3-one, $\mathbf{L^1}$, 6-(4-chloro-phenyl)-2H-pyridazine-3-one, $\mathbf{L^2}$ and s-triazine derivatives (2,4,6-

triamine-[1,3,5]-triazine, $\mathbf{L^3}$) and the salts $(NH_4)_6Mo_7O_{24}\cdot 12H_2O$ and $SnCl_2\cdot 2H_2O$, in concentrated hydrochloric acid (molar ratio Mo:Sn:**L** of 1:2:1) three complex compounds $(\mathbf{L^1}H)_2[MoOCl_4(SnCl_3)]$, **1**, $(\mathbf{L^2}H)_2[MoOCl_4(SnCl_3)]$, **2**, and $(\mathbf{L^3}H)_2[MoOCl_4(SnCl_3)]$, **3** have been prepared**.** These are monomeric species and they result as dark green-brown powders.

The syntheses were performed in the well established conditions regarding:

- molar ratio of Mo(VI) and Sn(II) salts used as starting materials Mo:Sn = 1:2
- *p*H of reaction medium: around 1
- temperature: 80-100^o C
- reaction time: 36 hours

Pyridazone and *s*-triazine derivatives ($\mathbf{L^1}$, $\mathbf{L^2}$ and $\mathbf{L^3}$) are weak basic ligands ($\mathbf{L^1}$ and $\mathbf{L^2}$ can act in both ceto (a) or enolic (b) forms) [12]. In the reaction medium (HCl) all the ligands ($\mathbf{L^1}$, $\mathbf{L^2}$ and $\mathbf{L^3}$) act as N-protonated monocations [18], $\mathbf{L}H^+$, (c) and (d):

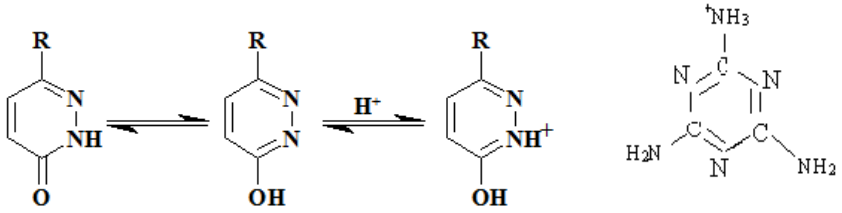

(a) **(b)** **(c)** **(d)**

3.2. Complex compounds characterization

The general formula of these compounds is supported by data from elemental analysis (Table 1), IR, UV/Vis and EPR spectra.

Table 1

Data from elemental chemical analysis

Compound	% Mo		% N		% Cl		% Sn	
	calc.	found	calc.	found	calc.	found	calc.	found
$(\mathbf{L^1}H)_2[MoOCl_4(SnCl_3)]$	11.27	9.87	6.57	6.08	29.18	30.28	13.97	14.15
$(\mathbf{L^2}H)_2[MoOCl_4(SnCl_3)]$	10.75	11.12	6.27	6.52	35.8	35.24	13.33	14.40
$(\mathbf{L^3}H)_2[MoOCl_4(SnCl_3)]$	13.08	13.39	11.45	10.01	33.87	34.45	16.22	15.45

L^{1} =6-p-tolyl-2H-pyridazine-3-one, **L**^{2}= 6-(4-chloro-phenyl)-2H-pyridazine-3-one and **L**^{3}= 2,4,6-triamine-[1,3,5]-triazine

Table 2

Electronic spectra of the compounds 1-3

Compound	$^2B_2 \rightarrow {}^2B_1$(I) λ(nm)/ν(kK)	$^2B_2 \rightarrow {}^2E$(II) λ(nm)/ν(kK)	$^2B_2 \rightarrow {}^2B_1$ λ(nm)/ν(kK)	$^2B_2 \rightarrow {}^2E$(I) λ(nm)/ν(kK)
(**L**^{1}H)$_2$[MoOCl$_4$(SnCl$_3$)]	270/33.00	360/27.70	430/23.20	700/14.20
(**L**^{2}H)$_2$[MoOCl$_4$(SnCl$_3$)]	265/38.00	360/27.70		680/14.70
(**L**^{3}H)$_2$[MoOCl$_4$(SnCl$_3$)]	295/33.90	360/27.70	430/23.20	700/14.20
BipyH$_2$[MoOBr$_5$]*	420/21.00			720/14.40

*compound used as comparison [14-16, 20], where Bipy is 2,2'-bipyridine

From Table 2 it results that the electronic spectra of compounds **1-3** exhibit *d-d* transitions specific for Mo^{5+}, (d^1);

$^2B_2 \rightarrow {}^2B_1$ ($d_{x^2-y^2}$ d_{xy}) ≈ 23000 cm^{-1}

$^2B_2 \rightarrow {}^2E_1$ ($d_{x^2-y^2}$ $d_{xz,}$ $d_{yz,}$) ≈ 15000 cm^{-1}

The position and shape of the absorption bands indicate a distorted octahedral geometry for these compounds [14-16, 20]. For comparison, in Table 2 the absorption bands of another complex with 2,2'-bipyridine (Mo(V) BipyH$_2$[MoOBr$_5$]) are given.

To provide additional data on the coordination type of these ligands the infrared spectra (IR) of complex compounds **1-3** and of the free ligands (**L**^{1} -**L**^{3}) have been also recorded (Table 3).

For complex compounds **1** and **2**, the bands from 1660-1670 cm^{-1}, 3100-3300 cm^{-1}, 770 cm^{-1} and 1510-1515 cm^{-1} were assigned to $\nu_{C=O,}$ $\nu_{NH,}$ $\nu_{CN\ aromatic}$ and $\nu_{C=Caromatic}$ vibrations, respectively. The bands from 1240 cm^{-1} or 1290 cm^{-1} were assigned to $\nu_{C\text{-}Ophenolic}$ vibration. Their presence confirms that the pyridazone derivatives **L**^{1} and **L**^{2} act as protonated ligands, **L**H^{+}.

Also in the case of compound **3**, the *s*-triazine derivative **L**^{3} acts as a protonated ligand, as it results from the shifting of N-H or C=N specific bands (ν_{NH}, ρ_{NH2}, $\delta_{NH2,}$ $\delta_{C=Ncycle}$) toward smaller frequencies, and from the presence of a new band at 2350 cm^{-1} assigned to streching frequencies ν_{NH+}.

For all complex compounds **1** – **3** the presence of the strong absorption bands in 990-1010 cm^{-1} range was assigned to the stretching frequencies $\nu_{Mo=O}$, specific for molybdenum-oxygen terminal group which exists in these compounds [14-16, 21].

The EPR spectra of the complex compouns **1 - 3** have similar shapes, and EPR parameters (Table 4). This proves the monomeric nature and distorted octahedral geometry of these compounds.

Table 3

Caracteristic bands in IR spectra for the ligands L^1 - L^3 and complex compounds 1 - 3

L^1	1	L^2	2	L^3	3	Assignment
460	-	460		460	-	δ_{C-N}
595	560	-		595	-	δ_{cycle}
-	-	-	-	630	640-660	γ_{NH2}
740	770	770	790	740	780	δ_{C-N}
820	-	810		820	-	δ_{cycle}
-	300	-	300	-	310	ν_{Sn-Cl}
-	990	-	980	-	980	$\nu_{Mo=O}$
-	420	-	420	-	440	ν_{Mo-Sn}
-	-	-	-	1200	1220	ρ_{NH2}
1380	1400	1390	1410	1380	1400	$\gamma_{C-N, cycle}$
1450	1440	1440	1450	1450	1440	δ_{cycle}
1590	1520	1550	1560	1520	1560	δ_{cycle}
-	-	-		1600	1620	δ_{NH2}, δ_{H-OH}
3210	3200	3500	3450	3200	3120	ν_{NH}, δ_{H-OH}

Table 4:

EPR data for the complex compounds 1 - 3

Complex	a_h	g_i
$(\mathbf{L^1}H)_2[MoOCl_4(SnCl_3)]$ **1**	64.5	1.945
$(\mathbf{L^2}H)_2[MoOCl_4(SnCl_3)]$ **2**	64.5	1.945
$(\mathbf{L^3}H)_2[MoOCl_4(SnCl_3)]$ **3**	64	1.94

3.2. Electrochemical characterization of complex compounds

Two complementary methods have been used for the electrochemical investigation. Differential pulse voltammetry (DPV) and cyclic voltammetry (CV) studies have been performed for each compound in acetonitrile with 0.1M tetrabutylammonium perchlorate (TBAP) as supporting electrolyte, in milimolar

solutions of $(\mathbf{L}^1H)_2[MoOCl_4(SnCl_3)]$, $(\mathbf{L}^2H)_2[MoOCl_4(SnCl_3)]$ and $(\mathbf{L}^3H)_2[MoOCl_4(SnCl_3)]$.

DPV study for each compound performed at different concentrations (0.5 – 3mM) enabled the measurement of anodic and cathodic peak potentials and currents for their redox processes. The CV study, performed at different concentrations (0.5 – 3mM), scan rates and potential ranges, enabled to establish the reversibility and irreversibility of these processes.

Results obtained by CV and DPV were in agreement concerning the peak potentials, and were complementary, yielding specific features for each process.

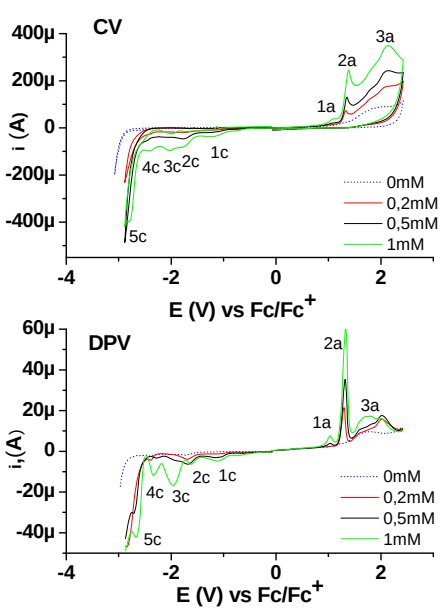

Fig. 1. CV and DPV curves for various concentrations of $(\mathbf{L}^1H)_2[MoOCl_4(SnCl_3)]$, **1**

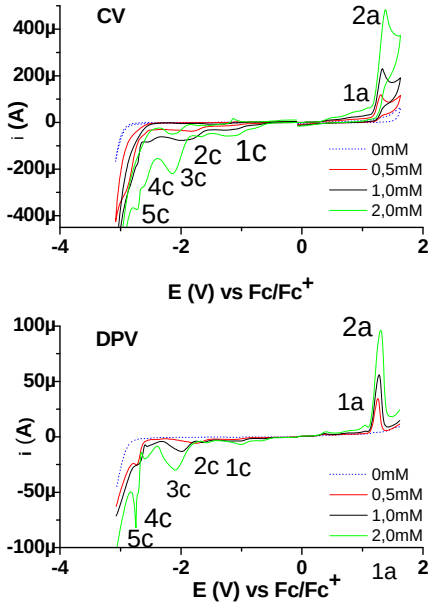

Fig. 2. CV and DPV curves for various concentrations of $(\mathbf{L}^2H)_2[MoOCl_4(SnCl_3)]$, **2**

Fig. 1 shows that both CV and DPV curves are influenced by the complex compound concentration, the currents increasing with the concentration of **1**. There are 3 anodic peaks (1a - 3a) and 5 cathodic peaks (1c - 5c). Fig. 2 shows the CV and DPV curves for the complex compound **2**. Their characteristics are similar to those for complex compound **1**. This confirms the complex compound similar structures, the differences being caused by the non similarity in the ligand structures.

Figs. 3 and 4, and respectively, 5 and 6, show that all redox processes of the complex compound **1** and **2** are irreversible. When comparing Fig 3 and 5 it

can be seen that at bigger complex compound concentration (1mM) a new peak (5c') appears in the reverse scan. It is the result of a process occurring at high cathodic potential (near the background evolution).

In Figs. 7 and 8 it is shown that both CV and DPV curves for complex compound **3** are influenced by the complex compound concentration, the currents being smaller than those obtained for complex compounds **1** and **2** due to the limited solubility of **3**. There are clearly seen only 2 anodic peaks (1a - 2a) and 2 large cathodic peaks (1c - 2c). In Fig. 7 it is shown that on both CV curves obtained at these low concentrations (0.2 and 0.4mM) there is a new peak (2c') at about -1V in the reverse scan, as in the case of the complex compound **2**. However, it appears when scanning to more negative potential values than for the compound **2**.

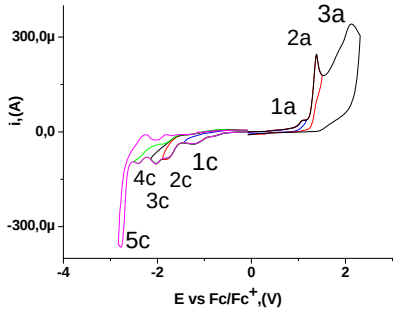

Fig. 3. CV curves at different scan ranges for **1**, [**1**] = 1mM in 0.1M TBAP, CH_3CN

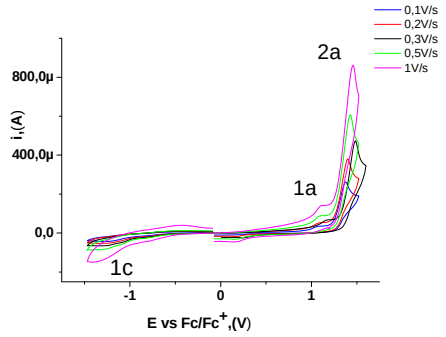

Fig. 4. CV curves at different scan rates for **1**, [**1**] = 1mM in 0.1M TBAP, CH_3CN

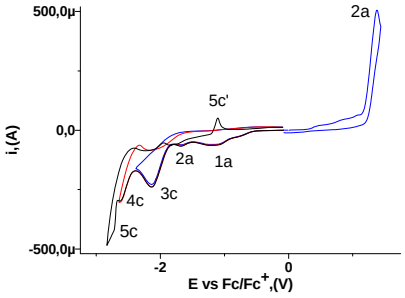

Fig. 5. CV curves at different scan ranges for 2, [2] = 2mM in 0.1M TBAP, CH_3CN

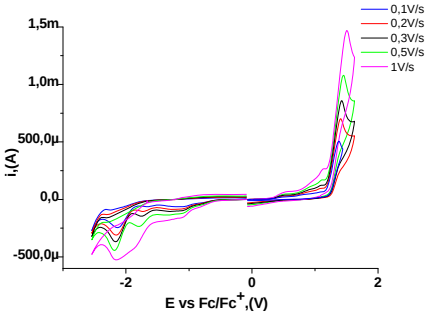

Fig. 6. CV curves at different scan rates for **2**, [**2**] = 2mM in 0.1M TBAP, CH_3CN

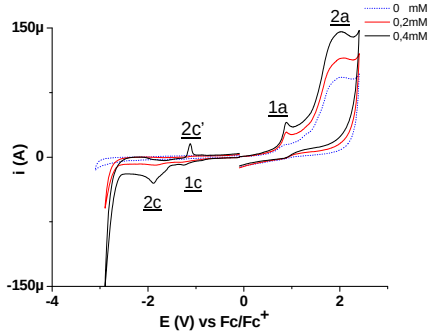

Fig. 7. CV curves for various concentrations of **3** in 0.1M TBAP, CH_3CN

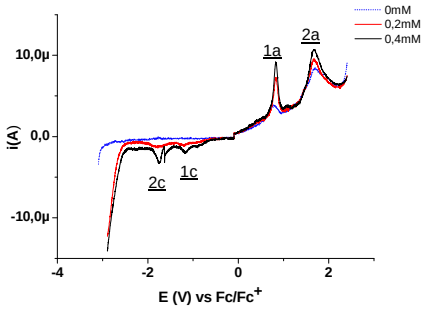

Fig. 8. DPV curves for various concentrations of **3** in 0.1M TBAP, CH_3CN

In Figs. 9 and 10 it is shown that all redox processes of the complex compound **3** are irreversible. Fig 10 also shows that all peaks (1c, 2c, 2c') increase with the scan rate.

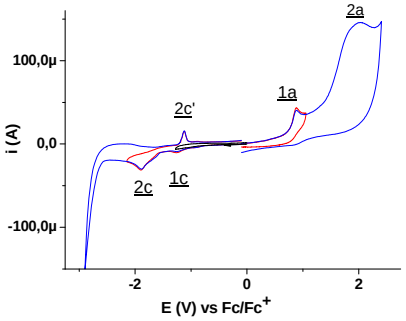

Fig. 9. CV curves at different scan ranges for $(\mathbf{L}^3H)_2[MoOCl_4(SnCl_3)]$, 0.4mM in 0.1M TBAP, CH_3CN

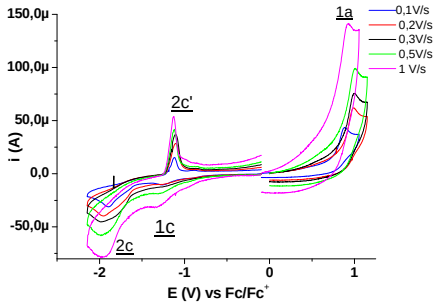

Fig. 10. CV curves at different scan rates for $(\mathbf{L}^3H)_2[MoOCl_4(SnCl_3)]$, 0.4mM in 0.1M TBAP, CH_3CN

The curves could be explained as follows: the cathodic processes for all these compounds occur with decomposition of the complex and metals deposition. The first reduction process could be attributted to the ligand reduction with complex decomposition. In the subsequent processes there are included the reduction of metal cations of tin, followed by molybdenum, to metals. The last processes are confirmed in the reverse scan by the appearance of sharp peaks characteristic to the dissolution of the freshly deposited metal layers. The anodic processes could be attributed to ligand oxidations.

4. Conclusion

A series of new complex compounds of molybdenum(V), $(\mathbf{L}H)_2[MoOCl_4(SnCl_3)]$ **1 – 3**, where the organic ligands were pyridazone and *s*–triazine derivatives: $\mathbf{L^1}$=6-p-tolyl-2H-pyridazine-3-one, $\mathbf{L^2}$ = 6-(4-chloro-phenyl)-2H-pyridazine-3-one and $\mathbf{L^3}$ = 2,4,6-triamine-[1,3,5]-triazine have been synthesized The compounds were obtained in hydrochloric acid (pH=1) starting from $(NH_4)_6Mo_7O_{24}\cdot 12H_2O$, $SnCl_2\cdot 2H_2O$, and the organic ligand, in the molar ratio of 1:2:1 (Mo:Sn:**L**). $SnCl_2$ acted not only as a reducing agent toward Mo(VI), used as starting material in the synthesis, but also as ligand; it is present in the coordination sphere as $SnCl_3^-$ unit. The complex compounds have monomeric structure as resulting from EPR data, and the organic ligand **L** acted as monoprotonated species, $\mathbf{L}H^+$ in all the obtained complex compounds. The spectral data (UV –Vis, IR and EPR) prove the distorted octahedral geometry of these new complexes. Complex compounds studies by cyclic voltammetry and differential pulse voltammetry show that all electrochemical processes are irreversible. The cathodic processes occur with decomposition of the complexes and metals deposition. After ligand reduction with complex decomposition the subsequent processes are the reduction of metal cations of tin, followed by molybdenum, to metals. The last processes are confirmed by the appearance of sharp peaks in the reverse scan, characteristic to the dissolution of the freshly deposited metal layers. The anodic processes have been attributed to ligand oxidations.

Aknowledgements

This work was supported by the strategic grant POSDRU/89/1.5/S/58852, Project „Postdoctoral programme for training scientific researchers” and POSDRU/88/1.5/S/60203 (COMPETE), cofinanced by the European Social Found within the Sectorial Operational Program Human Resources Development 2007 – 2013.

R E F E R E N C E S

[1] *A. Hroch, G. Gemmecker, W. R. Thiel,* Eur. J. Inorg. Chem., 2000, 1107
[2] *H. Balcar*, *D. Mishra*, *E. Marceau*, *X. Carrier*, *N. Zilkova*, *Z. Bastl*, Applied Catalysis A: General, 359, 2009, 129-135
[3] *S. Mathew, C. S. Kumara, N. Nagaraju*, Journal of Molecular Catalysis A: Chemical, 255, 2006, 243-248
[4] *J.M. Tunney, J.M. Master,* C.D. *Garner*, Comprehensive Coord. Chem. Elsevier, Amsterdam, 8, 2003, 459
[5] *D. Matoga, J. Szklarzewicz, K. Lewinski,* Polyhedron, 29, 2010, 94-99

[6] *S. Gupta, S. Pal, A. K. Barik, S. Roy, A. Hazra, T. N. Mandal, R. Butcher, S. K. Kar*, Polyhedron, 28, 2009, 711-720
[7] *C. N. Malele, J. Ray, W. E. Jones Jr.* Polyhedron, 29, 2010, 749-756
[8] *V. Vrdoljak, D. Milic, M. Cindric, D. Matkovic-Calogovic, D. Cincic*, Polyhedron, 26, 2007, 3363-3372
[9] *Q. Zhang, K. Starke, C. Schulzke, A. Hofmeister, J. Magull,* Inorganica Chimica Acta 360, 2007, 3400-3407
[10*J R. A. Lal, D. Basumatary, S. Adhikari, A. Kumar*, Spectrochimica Acta Part A 69, 2008, 706-714
[11] *M. J. Morris,* Coordination Chemistry Reviews 138, 1995, 121
[12] *M. J. Morris*, Coordination Chemistry Reviews 172, 1998, 181
[13] *I.Topaloglu-Sozuer, A. Gunyar., S. Dulger-Irdem, M. Baya, R. Poli*, Inorganica Chimica Acta 358, 2005, p. 3303
[14] *C. Gheorghiu, C. Guran*, Rev. Chim., 35(12), 1984, 1085
[15] *C. Gheorghiu, C. Guran, A. Meghea*, Rev. Chim., 33(8), 1982, 741
[16]. *C. Gheorghiu,C. Guran, A. Meghea*, Revue Roumaine de Chimie, 29(9-10), 1984, 747
[17]. *M. Micu, M.Dinculescu*, Sci. Bull. UPB, Series B, 60(1-2), 1998, 53
[18]. *H. Chivu, B. Calmuschi-Cula, N. Stanica, O. Micu, C. Guran*, Rev. Chim. (Bucureşti), 57 (7), 2006, 735
[19]. *H. Chivu, B. Braun, O. Micu, C. Guran*, Rev. Chim. (Bucureşti), Rev. Chim. (Bucureşti), 62 (3), 2011, 283
[20]. *A. B. P. Lever,* Inorganic Electronic Spectroscopy, Elsevier Publ. Comp., Amsterdam, London, New York, 1984
[21] *K. Nakamoto*, Infrared Spectra of Inorganic and Coordination Compounds, Willey Interscience, 1970.